



Search for CP violation in the phase space of $D^0 \rightarrow \pi^- \pi^+ \pi^0$ decays with the energy test

LHCb collaboration[†]

Abstract

A search for CP violation in $D^0 \rightarrow \pi^- \pi^+ \pi^0$ decays is reported, using pp collision data collected by the LHCb experiment from 2015 to 2018 corresponding to an integrated luminosity of 6 fb^{-1} . An unbinned model-independent approach provides sensitivity to local CP violation within the two-dimensional phase space of the decay. The method is validated using the Cabibbo-favoured channel $D^0 \rightarrow K^- \pi^+ \pi^0$ and background regions of the signal mode. The results are consistent with CP symmetry in this decay.

Published in JHEP 09 (2023) 129

© 2024 CERN for the benefit of the LHCb collaboration. CC BY 4.0 licence.

[†]Authors are listed at the end of this paper.

1 Introduction

In the Standard Model (SM) of particle physics, CP violation is included in the quark sector through a single weak phase in the CKM matrix [1, 2]. While this satisfies one of the Sakharov conditions required for baryogenesis [3], the baryon asymmetry observed in the universe exceeds by several orders of magnitude the level accommodated within the SM [4, 5]. This motivates the search for physics beyond the SM and makes CP -violation studies a promising direction in this search. In the kaon and beauty sectors, CP violation has been long established [6–15]. However, it was only in 2019 that a statistically significant observation of CP violation was made in charm hadrons, by the LHCb collaboration [16].

There is currently no clear consensus whether the observed level of CP violation in charm hadrons can be accommodated within the SM, due to the challenges of performing calculations of asymmetries in charm decays [17–22]. In the SM, charm CP violation is expected to be small due to a combination of CKM suppression and GIM cancellation. Depending on the decay mode, it is predicted to reach $\mathcal{O}(10^{-3})$, with the largest effects in singly Cabibbo-suppressed (SCS) channels, where CP violation appears via interference between tree and penguin amplitudes with different strong and weak phases [23–25]. Multi-body charm decays provide a powerful tool to probe CP violation. In these decays, phase-space-dependent local CP asymmetries can arise from the interference among intermediate resonances, which leads to a corresponding variation of strong phases. Studies of these local asymmetries provide additional sensitivity to observation of CP violation, complementing studies of phase-space integrated asymmetries and two-body decays [26–30]. Similar investigations in the beauty sector have revealed very large local asymmetries, approaching 100% in magnitude for some phase-space regions [31, 32].

In charm quark decays, CP violation was discovered by measuring the difference in time-integrated CP asymmetries of the two-body decays $D^0 \rightarrow K^+K^-$ and $D^0 \rightarrow \pi^+\pi^-$, to construct the quantity ΔA_{CP} [16]. Recently, a dedicated LHCb measurement of the CP asymmetry in $D^0 \rightarrow K^+K^-$ decays was performed. In conjunction with ΔA_{CP} , this indicates that the observed CP violation is driven by an asymmetry in the $\pi^+\pi^-$ decay mode, at greater than 3σ significance [33]. The three-body SCS decay $D^0 \rightarrow \pi^-\pi^+\pi^0$ is dominated by $D^0 \rightarrow \rho^\pm\pi^\mp$ amplitudes, which proceed via the same quark-level transitions as the decay $D^0 \rightarrow \pi^+\pi^-$. A previous LHCb search for local CP violation in this decay measured a p -value of 2.6% for the hypothesis of CP symmetry [34] and the world average of the phase-space integrated asymmetry is in agreement with CP symmetry [35–38]. The third most important amplitude of the $D^0 \rightarrow \pi^-\pi^+\pi^0$ decay, $D^0 \rightarrow \rho^0\pi^0$, shares the weak structure with the two-body decay $D^0 \rightarrow \pi^0\pi^0$, whose world-average CP asymmetry is also in agreement with CP symmetry [39–41].

In this paper, a search for local CP violation in the decay $D^0 \rightarrow \pi^-\pi^+\pi^0$ is performed using LHCb data collected during LHC Run 2 from 2015–2018. An unbinned model-independent method called the energy test [42–45] is used to determine a p -value quantifying compatibility with the null hypothesis of CP symmetry. The method follows that used in the predecessor LHCb analysis [34].

2 Analysis overview

The energy test [42–45] is an unbinned statistical test to compare two distributions and quantify their agreement with being drawn from a common source, making it appropriate for comparing signal distributions in multidimensional phase space of particle decays. The test has been used in several previous LHCb searches for CP violation [34, 46, 47]. In this analysis the energy test is used to compare samples of D^0 and \bar{D}^0 mesons decaying to the $\pi^-\pi^+\pi^0$ final state. The test is insensitive, by construction, to any global charge asymmetries present in the sample. It provides a single p -value quantifying consistency with the CP symmetry hypothesis. This analysis benefits from several improvements in the technique, which reduce the computational requirements and hence enable the test to be applied to much larger data samples than was previously feasible [48–50].

A sample of flavour-tagged $D^0 \rightarrow \pi^-\pi^+\pi^0$ decays is obtained by selecting D^{*+} candidates that decay via $D^{*+} \rightarrow D^0(\rightarrow \pi^-\pi^+\pi^0)\pi^+$.¹ The charge of the low-momentum (soft) pion from the D^{*+} decay is used to identify the flavour of the accompanying D^0 candidate. The analysis methods are developed and validated using three independent approaches: realistic pseudoexperiment simulations with and without CP asymmetries injected; studies of a topologically similar control mode in collision data, where CP violation is expected to be negligible; and studies with the signal mode following randomisation of the charm meson flavour and injection of fake asymmetries to mimic nuisance effects from production and detection asymmetries. After all methods are validated the energy test is performed in the signal channel to search for CP asymmetries.

For a three-body meson decay with spinless initial and final states, the phase space is fully defined by two kinematic quantities. In this analysis, the Dalitz-plot formalism is used to describe the signal decay using squared invariant masses of two-body combinations of final state particles. To enable a direct comparison of the Dalitz plane distributions for D^0 and \bar{D}^0 decays, a set of flavour-symmetric coordinates is defined: $s_{12} \equiv m^2(\pi^\pm\pi^\mp)$, $s_{13} \equiv m^2(\pi^\pm\pi^0)$, and $s_{23} \equiv m^2(\pi^\mp\pi^0)$, where in all cases the upper (lower) charge superscript refers to the D^0 (\bar{D}^0) case.

To assess the impact of experimental effects such as production and detection asymmetries, the Cabibbo-favoured (CF) decay $D^0 \rightarrow K^-\pi^+\pi^0$ is used as a control channel, which is topologically and kinematically similar to the signal decay. The CF channel benefits from a yield approximately eight times greater than the signal. This enables the control mode to be split into several independent samples with signal-like yields to test for biases from detector-induced asymmetries. Wherever possible, the event selection for the control mode is chosen to match the corresponding signal selection. The main difference between the signal and control modes is the presence of a charged kaon in the control mode. Due to material effects in the detector, $K^-\pi^+$ detection asymmetries are known to be much larger than for $\pi^+\pi^-$ [51], so the signal mode is anticipated to suffer from smaller nuisance asymmetries than the control mode.

3 LHCb experiment

The LHCb detector [52, 53] is a single-arm forward spectrometer covering the pseudorapidity range $2 < \eta < 5$, designed for the study of particles containing b or

¹Unless stated otherwise, the charge conjugate mode is implicit throughout.

c quarks. The detector includes a high-precision tracking system consisting of a silicon-strip vertex detector surrounding the pp interaction region [54], a large-area silicon-strip detector located upstream of a dipole magnet with a bending power of about 4 Tm, and three stations of silicon-strip detectors and straw drift tubes [55] placed downstream of the magnet. The tracking system provides a measurement of the momentum, p , of charged particles with a relative uncertainty that varies from 0.5% at low momentum to 1.0% at 200 GeV/ c . The minimum distance of a track to a primary pp collision vertex (PV), the impact parameter (IP), is measured with a resolution of $(15 + 29/p_T)$ μm , where p_T is the component of the momentum transverse to the beam, in GeV/ c . Different types of charged hadrons are distinguished using information from two ring-imaging Cherenkov detectors [56]. Photons, electrons and hadrons are identified by a calorimeter system consisting of scintillating-pad and preshower detectors, an electromagnetic and a hadronic calorimeter. Muons are identified by a system composed of alternating layers of iron and multiwire proportional chambers [57]. The online event selection is performed by a trigger [58], which consists of a hardware stage based on information from the calorimeter and muon systems, followed by a software stage which applies a full event reconstruction.

The neutral pion candidate in the $D^0 \rightarrow \pi^- \pi^+ \pi^0$ final state is reconstructed from its diphoton decay based on energy deposits in the electromagnetic calorimeter. The reconstructed neutral pions can be separated into two categories, depending on the opening angle between the photons produced in the $\pi^0 \rightarrow \gamma\gamma$ decay. A π^0 candidate is labelled *resolved* if the decay photons are reconstructed as two distinct electromagnetic calorimeter clusters and as *merged* if the two photons are reconstructed as a single cluster [53]. The two categories differ mainly in the kinematics of the neutral pion (merged π^0 candidates tend to have higher momentum than resolved) and therefore the reconstructed Dalitz distributions for the two types are also quite different. To maximise the sensitivity to potential CP violation effects over the entire phase space, the two categories are combined before applying the energy test. However, the event selection is optimised separately for the two categories to reflect their different characteristics.

4 The energy test method

In this analysis, the energy test method is used to compare the Dalitz distributions of D^0 and \bar{D}^0 meson decays to provide a sensitive search for CP violation within the phase space of these decays. The test quantifies localised sample differences by calculating a single test statistic defined as

$$T \equiv \frac{1}{2n(n-1)} \sum_{i,j \neq i}^n \psi_{ij} + \frac{1}{2\bar{n}(\bar{n}-1)} \sum_{i,j \neq i}^{\bar{n}} \psi_{ij} - \frac{1}{n\bar{n}} \sum_{i,j}^{n,\bar{n}} \psi_{ij}.$$

The function ψ_{ij} depends on the distance between pairs of candidates in the phase space, d_{ij} , such that $\psi_{ij} = \psi(d_{ij})$. The first double summation is over all possible pairs of (n) D^0 candidates, the second is over all pairs of (\bar{n}) \bar{D}^0 candidates, while the third is over all D^0 - \bar{D}^0 pairs. The normalisation of each term removes any effects from global asymmetries, such that by construction only local asymmetries are probed in the energy test. Under the null hypothesis that the two samples are drawn from the same underlying distribution, the T -value is drawn from a distribution around zero. In the presence of differences between

the two samples, as might be caused by CP violation [42–45], the T distribution shifts to larger values.

For this analysis, ψ_{ij} is chosen to be a Gaussian function $\psi_{ij} = e^{-d_{ij}^2/2\delta^2}$, and the distance between candidate pairs is defined symmetrically in terms of the three squared invariant masses of two-pion combinations, $d_{ij}^2 = [(\Delta s_{12})_{ij}^2 + (\Delta s_{13})_{ij}^2 + (\Delta s_{23})_{ij}^2]$, where $(\Delta s)_{ij}$ gives the difference in the coordinate s for candidates i and j . The tunable parameter δ constrains the effective radius in phase space within which local asymmetries can be probed. Its value is optimised to maximise sensitivity to CP violation as discussed in Sec. 6.

The calculated T -value can be converted into a p -value by comparing it to the distribution expected under the null hypothesis. This distribution is determined by running the test repeatedly where candidates of both flavours are randomly assigned to the two samples. The fraction of these permutation tests with T -values greater than the value under test then sets the p -value of the overall test. The distribution of T under the null hypothesis scales directly with the sample size [48–50], so can be determined using significantly smaller samples than used for the nominal result.

5 Event selection

This analysis uses proton-proton collision data corresponding to an integrated luminosity of approximately 6 fb^{-1} , collected during the LHC Run 2 period (2015–2018) at a centre-of-mass energy $\sqrt{s} = 13 \text{ TeV}$.

At the hardware trigger stage, signal $D^0 \rightarrow \pi^- \pi^+ \pi^0$ events are selected either through significant energy deposits in the hadronic calorimeter (associated with one or both of the charged pions from the D^0 decay), or through deposits in the electromagnetic calorimeter consistent with a photon shower (associated with the neutral pion decay). Other events passing the hardware trigger are also selected if the trigger decision is independent of the signal candidate.

At the first stage of the software trigger a partial event reconstruction is performed. Candidates are selected if they satisfy either of two multivariate displaced track algorithms. The first accepts a single track if it fulfils a two-dimensional requirement for minimum values in $(p_T, \chi_{\text{IP}}^2)$ space, where χ_{IP}^2 is the difference in the χ^2 of the PV fit with and without the track under consideration. This algorithm preferentially accepts tracks with large values of p_T, χ_{IP}^2 , or both. The second is a two-track algorithm utilising several variables within a boosted decision tree, sensitive to track pairs produced at a significant distance from the PV.

At the second software trigger stage, a full event reconstruction is performed taking into account the best available knowledge of detector alignment and calibration. Candidates must pass either dedicated channel-specific triggers, or an inclusive topological trigger. The latter exploits the characteristic signature $D^{*+} \rightarrow D^0 \pi^+$ with $D^0 \rightarrow h^+ h'^- X$, where h represents any charged long-lived hadron and X indicates unreconstructed decay products.

Following the trigger stage, the offline selection starts with the reconstruction of D^0 candidates. The two charged pions from the D^0 decay must be significantly displaced from the PV and fulfil particle identification requirements to remove backgrounds from kaons and incorrectly reconstructed tracks (ghosts). The two pions must form a good-quality vertex and have an invariant mass below $1850 \text{ MeV}/c^2$. The neutral pion must be identified

using dedicated LHCb algorithms via resolved or merged photon signatures, and the diphoton system must have an invariant mass consistent with the known π^0 mass. A D^0 candidate is then reconstructed from the combination of the neutral pion and two charged pions. The three-particle system must have an invariant mass consistent with the known mass of the D^0 meson. The direction of the D^0 momentum vector is required to be consistent with that of the displacement vector joining the production and decay vertices.

To reconstruct the D^{*+} candidate, an additional charged pion is combined with the D^0 meson. This soft pion is subject to particle identification requirements to remove backgrounds from ghost tracks and misidentified particles, and must be consistent with originating at the PV. The $D^0\pi^+$ system is required to have a good vertex quality and a reconstructed mass difference $\Delta m \equiv m(D^{*+}) - m(D^0)$ less than $180 \text{ MeV}/c^2$.

When reconstructing the decay a kinematic refit of the full D^{*+} decay chain is performed to improve the resolution with externally imposed constraints [59]. The D^{*+} candidate is constrained to originate from the PV, and the π^0 candidate is mass-constrained to the known experimental value. When calculating the Dalitz variables used as inputs to the energy test, there is an additional requirement constraining the reconstructed mass $m(\pi^-\pi^+\pi^0)$ to the known D^0 mass, which ensures that candidates lie in the physically allowed kinematic region.

Potential contamination from clone tracks, corresponding to single charged particles reconstructed as multiple near-collinear tracks, is efficiently suppressed by requiring that all pairs of tracks have an angular separation exceeding 0.0005 rad .

After the offline selection procedure, the dominant background remaining in the sample corresponds to random combinations of tracks and neutral pions. This background is significantly higher for the resolved π^0 channel, due to the low- p_T diphoton signature. To further suppress this background a multivariate classifier is developed and applied to the resolved channel alone. The figure-of-merit to be maximised is the quantity $S/\sqrt{(S+B)}$, where S (B) is the signal (background) yield within the signal region defined by $|\Delta m - 145.4| < 1.8 \text{ MeV}/c^2$. The multivariate selection gives an appreciable gain in signal significance for the resolved channel, while no corresponding improvement is found when applying a similar approach for the merged channel.

A boosted decision tree (BDT) classifier is trained and tested using data, based on the TMVA framework [60]. The signal (background) sample is formed of $D^0 \rightarrow \pi^-\pi^+\pi^0$ candidates each with a signal (background) weight determined using the *sPlot* technique [61] with Δm as the discriminating variable. To avoid biases from the BDT training, the data are divided into two disjoint halves such that the classifier trained on one half is applied to the second half and vice versa.

After applying all selection criteria, a small fraction of events contain more than one signal candidate. These may affect the present analysis, as they can lead to candidates with identical or near-identical phase-space coordinates. As a precaution to mitigate potential biases in the energy test, a single candidate is randomly chosen to be retained in such cases. This affects approximately 3% (6%) of events in the merged (resolved) samples.

The Δm distributions after applying all selection criteria are shown in Fig. 1. These distributions are fitted to obtain signal and background yields for use in sensitivity studies, as described later. For these fits the signal peaks are modelled by the sum of three Gaussian functions, where for the resolved sample one of them has different width parameters for the left and right halves of the peak. The background is described by an empirical threshold

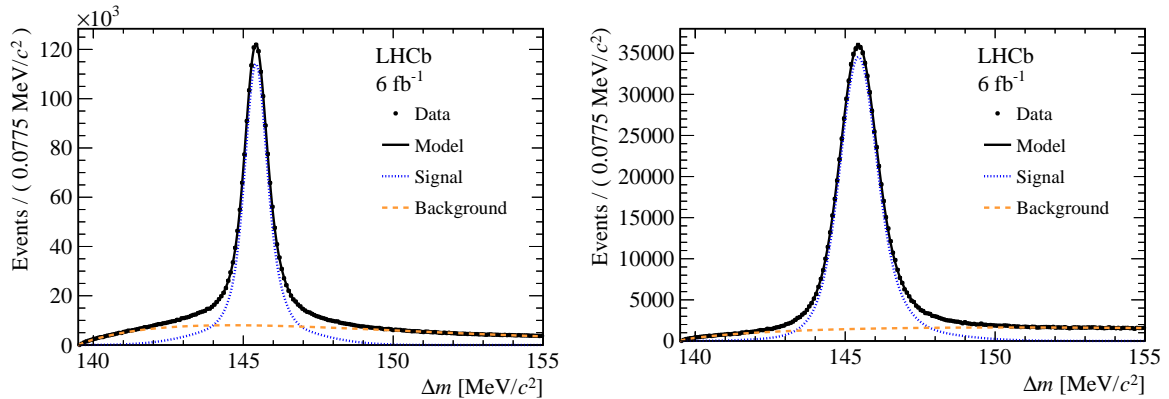


Figure 1: Distributions of Δm for (left) the resolved and (right) merged π^0 samples after the application of all selection criteria except the Δm requirement. Also shown are projections of the fit model used to evaluate signal yields and purity.

shape $F_{\text{bkg}}(x) = (x - x_0)^\alpha e^{-\beta(x-x_0)}$, with α and β freely varying in the fit and with x_0 fixed to the known mass of the charged pion. All free parameters for both signal and background models are independent for the merged and resolved samples.

When applying the energy test, only candidates within the region $|\Delta m - 145.4| < 1.8 \text{ MeV}/c^2$ are used. This yields a sample of 1.71M (0.76M) signal decays with a purity of 81% (91%) for the resolved (merged) sample. This exceeds by more than a factor of four the signal yield of the corresponding LHCb Run 1 analysis [34].

The control channel $D^0 \rightarrow K^- \pi^+ \pi^0$ is selected using the same criteria except for the particle identification requirements on the kaon and pion, which result in mutually exclusive samples for the signal and control modes. The kinematic distributions of the final state particles are similar for the selected signal and control mode data. The yield of the control mode is 5.32M (13.78M) for the merged (resolved) π^0 samples, with a purity of 97% (94%).

To suppress the potential impact of nuisance asymmetries, the number of candidates collected in each of the two LHCb dipole magnet polarities is equalised by randomly rejecting candidates from the larger sample. This mitigates against potential instrumental asymmetries due to geometrical effects, whereby particles of a particular charge are more likely to be swept out of the acceptance. The equalisation improves the cancellation of such effects at the cost of around 5% reduction in signal yield. The equalisation is enforced independently for each of the four data-taking years (2015–2018) to reflect different conditions, for both signal and control modes.

The background-subtracted Dalitz distributions for the resolved and merged π^0 categories are shown in Fig. 2. Three $\rho^{\pm,0}$ resonances are clearly visible as two-lobe structures in the Dalitz plane. These dominate the phase space, as expected from previous studies [62]. Candidates with large values of s_{12} , corresponding to the lower left corner of the Dalitz plane, have little remaining centre-of-mass energy for the neutral pion. As such, this region of phase space is dominated by resolved (low momentum) π^0 candidates.

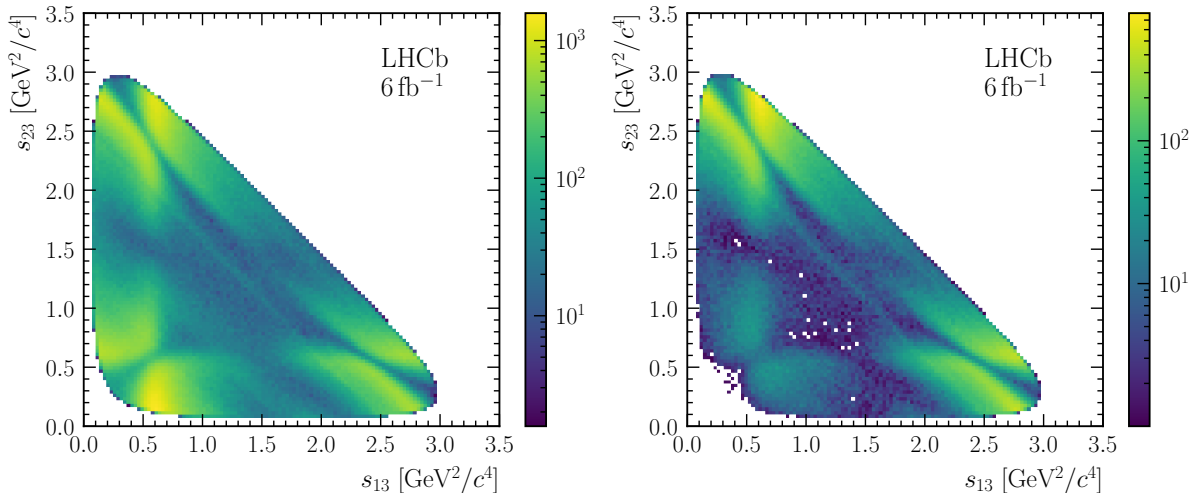


Figure 2: Dalitz plots for the background-subtracted signal samples for (left) the resolved and (right) merged π^0 categories, with the two $m^2(\pi^\pm\pi^0)$ variables chosen for the projection. The three $\rho^{\pm,0}$ resonances dominate the phase space.

6 Sensitivity studies and optimisation

The energy test has a single tunable parameter, δ , which sets the phase-space scale of the test and is chosen to optimise the sensitivity of the method. The optimal value depends on the size of the dataset and the distribution of candidates in the phase space. Different values chosen for δ may be optimal for different CP violation scenarios. Pseudoexperiments are used to study such effects and select the δ value for this analysis.

In the pseudoexperiments, phase-space distributions of signal decays are generated using the LAURA⁺⁺ package [63], with an amplitude model taken from a previous analysis of this channel [62]. This model consists of several components from different intermediate resonances and a non-resonant term, each multiplied by a complex coefficient. The dominant contributions are from charged and neutral $\rho(770)$ resonances, with fit fractions of 67.8% ($\rho^+\pi^-$), 34.6% ($\rho^-\pi^+$), and 26.2% ($\rho^0\pi^0$) for the D^0 decay. The D^0 and \bar{D}^0 complex coefficients, either in their magnitudes or phases, are adjusted for both the dominant ($\rho(770)^+\pi^-$) and sub-dominant ($\rho(770)^-\pi^+$) intermediate states to emulate CP -violation.

For each pseudoexperiment the number of signal candidates is set to match the corresponding signal yield in data, for the combination of merged and resolved samples. Nonuniform efficiency effects and background contamination are implemented based on studies with the data to make the pseudoexperiments more realistic. The efficiency variation across the Dalitz plane is estimated by comparing background-subtracted data with the generator-level simulation. It is found to vary smoothly over the Dalitz plane, with around 10% variation across the two $m^2(\pi^\pm\pi^0)$ variables, and decreasing by around 50% from low to high $m^2(\pi^+\pi^-)$. For different studies, backgrounds are generated either with or without a global charge asymmetry.

Pseudoexperiments are generated with CP asymmetries of varying size to study the sensitivity of the analysis as a function of the choice of δ value. Phase (magnitude) differences between D^0 and \bar{D}^0 decay amplitudes are generated in the range 0.1° – 1.0° (0.1%–1.0%). These pseudoexperiments are evaluated using the energy test method

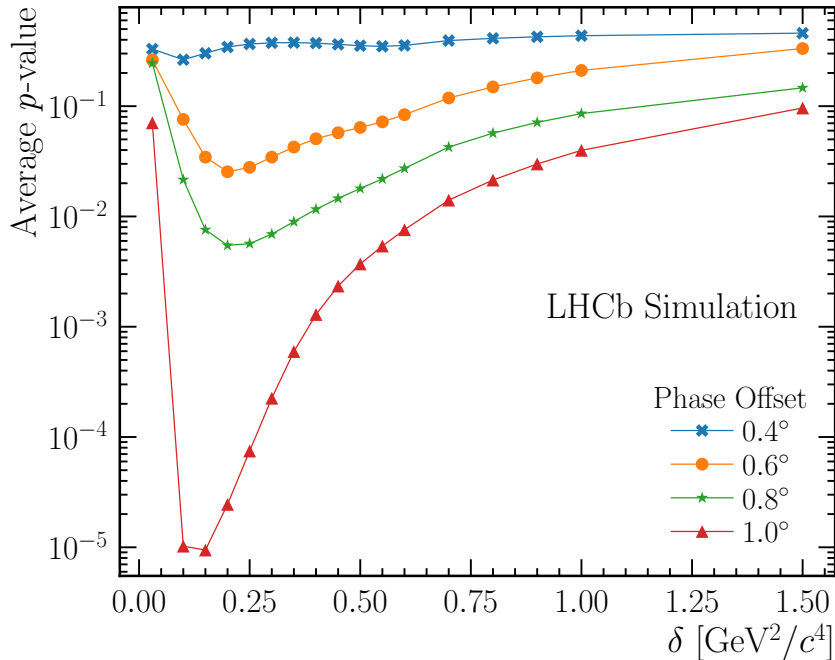


Figure 3: Average p -value as a function of the energy test distance parameter δ , for different values of the D^0 - \bar{D}^0 phase difference for the $D^0 \rightarrow \rho(770)^- \pi^+$ amplitude. Straight guide lines are also drawn connecting successive points for each scenario.

at 17 different values of δ ranging from 0.03–1.5 $(\text{GeV}/c^2)^2$. In each case a p -value is determined and these are plotted as a function of δ . The optimal choice of δ for a given pseudoexperiment is that which gives the smallest p -value. To reduce the impact of statistical fluctuations, five pseudoexperiments are generated for each CP violation scenario and the average p -value is calculated for each point in the scan. An example of this procedure is presented in Fig. 3, which shows the δ scans for different phase differences injected into the sub-dominant $D^0 \rightarrow \rho(770)^- \pi^+$ amplitude. The minimum p -value is found close to $\delta = 0.2 (\text{GeV}/c^2)^2$ for all cases, hence this is chosen as the distance parameter for the energy test throughout this analysis.

To assess the overall sensitivity for a particular CP asymmetry scenario, an ensemble of 500 pseudoexperiments is generated with a phase difference of 0.9° in the dominant $D^0 \rightarrow \rho(770)^+ \pi^-$ amplitude. The significance of the result, expressed as a one-sided Gaussian z -score, follows a Gaussian distribution with a mean of 4.3σ and a width of 0.7σ . If nature exhibited a CP asymmetry of this type, this analysis would obtain a 3σ evidence in 95% of cases. Similar sensitivity studies indicate that the energy test applied to the current sample is insensitive to CP phase asymmetries below 0.5° and to magnitude asymmetries below 0.5%, for the two specific amplitudes investigated. Should a significant CP asymmetry be observed, a more complete amplitude analysis would be needed to fully understand the results.

7 Validation and cross-checks using data

Several checks are performed with data to assess the potential impact of nuisance asymmetries on this analysis and confirm that the reported p -value is unbiased. This section describes studies using the control mode, background-dominated samples, and pseudo-experiments produced with the signal data sample with flavour information removed and different nuisance asymmetries injected. These studies demonstrate that any local nuisance asymmetries which might affect the signal decay mode are sufficiently small that they can be neglected without impacting the results. There are global asymmetries of order 1%, but these do not vary significantly over the Dalitz plane.

For the control mode $D^0 \rightarrow K^-\pi^+\pi^0$, the combined sample with both π^0 meson types contains approximately 19 million candidates after all selection requirements are imposed. The fraction of merged π^0 candidates is 27%, consistent with the 26% fraction for the signal mode. The energy test is evaluated on eight independent, randomly chosen subsamples of the control mode data, each having a yield approximately matching that in the signal channel. The eight resulting p -values are consistent with having been drawn from a uniform distribution between zero and one, indicating that any nuisance asymmetries from production or detector effects are small enough to be neglected in the signal channel.

Here and elsewhere, the agreement of the set of p -values, p_i , with being drawn from a uniform distribution is tested by calculating the statistic $P = -2 \sum_{i=1}^N \log p_i$. The P -statistic follows a χ^2 distribution with $2N$ degrees of freedom if the individual p -values are sampled from a uniform distribution. Hence, a value of $P/2N$ significantly greater than unity would be indicative of a nonuniform distribution.

For the eight-sample test over the control mode, no evidence is found of any deviation from a uniform p -value distribution, with $P/2N = 16.4/16$. A further test is performed with a division into four subsamples, each with twice the signal yield. Again, no indication of non-uniformity is observed ($P/2N = 10.3/8$). This confirms that this method is insensitive to existing nuisance asymmetries even with double the sample size currently available.

Charge asymmetries in background candidates may be present and can in principle bias the energy test if they vary across the phase space. To supplement the control mode checks in the signal Δm region, the energy test is also performed in background-dominated Δm sidebands for both signal and control modes. This region is defined as the union of the ranges ($\Delta m < 142 \text{ MeV}/c^2$) and ($150 < \Delta m < 155 \text{ MeV}/c^2$). Evaluating the energy test using the 810k candidates in this region of the signal channel gives a p -value of 0.57. In the control mode a set of three sideband samples are defined, each with a similar yield to the signal mode sideband sample, with none giving a p -value below 0.2 from the energy test. Hence, there is no indication that background asymmetries are biasing this analysis, with the current sample sizes.

To supplement the above studies, a suite of checks are performed using the signal sample. Flavour-randomised pseudoexperiments are produced by randomly labelling each signal candidate as D^0 or \bar{D}^0 . These CP -symmetric pseudoexperiments are then injected with nuisance asymmetries of various types, by suitably rejecting candidates according to their assigned flavour. By running the energy test over large ensembles of such samples, the potential bias from these nuisance asymmetries on the measured p -value can be quantified with higher confidence than the control mode studies, which are limited to at most eight independent subsamples.

For each type of nuisance asymmetry to be investigated, the first step is to use external inputs to construct binned asymmetry maps as a function of the signal particle kinematics. These asymmetries are then injected into the flavour-randomised samples. The realistic nuisance asymmetries are determined using a sample of $D^{*+} \rightarrow D^0(\rightarrow K_S^0\pi^-\pi^+)\pi^+$ decays, where no significant CP violation is expected. The selection of this channel is aligned where possible with the $D^0 \rightarrow \pi^-\pi^+\pi^0$ signal mode, resulting in around 12M signal candidates with 96% purity within the selected Δm range. From this sample, the raw asymmetry in D^0 versus \bar{D}^0 candidates is determined as a function of the reconstructed kinematic variables for different particles.

Nuisance asymmetries are determined as a two-dimensional map of the soft pion transverse momentum and pseudorapidity. While a significant global asymmetry is observed of around -0.9% , there is little indication of any trend across the kinematic distributions. Using this map to generate an ensemble of asymmetry-injected flavour-randomised signal samples, and running the energy test over each one, a p -value distribution is obtained and found to be consistent with being uniform between zero and one ($P/2N = 98/100$). This study is extended to inject polarity-specific asymmetries and again the p -values are consistent with being uniformly distributed ($P/2N = 205/200$).

Injecting asymmetries as a function of the soft pion kinematics, as described above, is found to account for possible asymmetry dependence on kinematics of other particles in the decay chain. This is checked by comparing appropriate asymmetry maps from the $D^0 \rightarrow K_S^0\pi^-\pi^+$ channel with those from pseudoexperiments injected with asymmetries based on soft pion kinematics alone. As an additional check, asymmetries are injected as a function of (p_T, η) for the two pions from the D^0 decay. Again, no evidence is found for any bias in the p -value evaluation.

In addition to checking p -value distributions of independent pseudoexperiments for uniformity, the same procedure is used to assess potential biases in the p -value from a single pseudoexperiment, when it is repeatedly and independently subjected to the asymmetry injection. For such checks, the significance (z -score) for the flavour-randomised sample is compared to the distribution of significances obtained after injecting asymmetries. This process is repeated several times to assess potential biases. The observed shifts in significance are generally consistent with Gaussian distributions centred at zero, with a few cases where a small but significant mean shift is observed of up to 0.1σ (in both directions). The overall conclusion of these studies is that the energy test is robust against any potential nuisance asymmetries in the signal sample.

As further cross-checks, the energy test is evaluated separately using subsamples of the control mode defined according to the data-taking year and in three disjoint categories according to the type of hardware trigger satisfied by the event. Subsamples are also defined by splitting into ranges of soft pion or D^0 transverse momentum or pseudorapidity. No significant p -values are obtained, except when requiring that the hadronic hardware trigger is satisfied by one or both of the charged hadrons (K^- or π^+) from the D^0 decay. In that case p -values below 1% are found for both such subsamples with signal-like yields. If the category is redefined such that the charged pion must by itself satisfy the hadronic trigger, no significant p -values are obtained. Hence we conclude that this bias is caused by the charged kaon, which is known to be associated with larger nuisance asymmetries from material interaction effects, and which is absent in the signal mode.

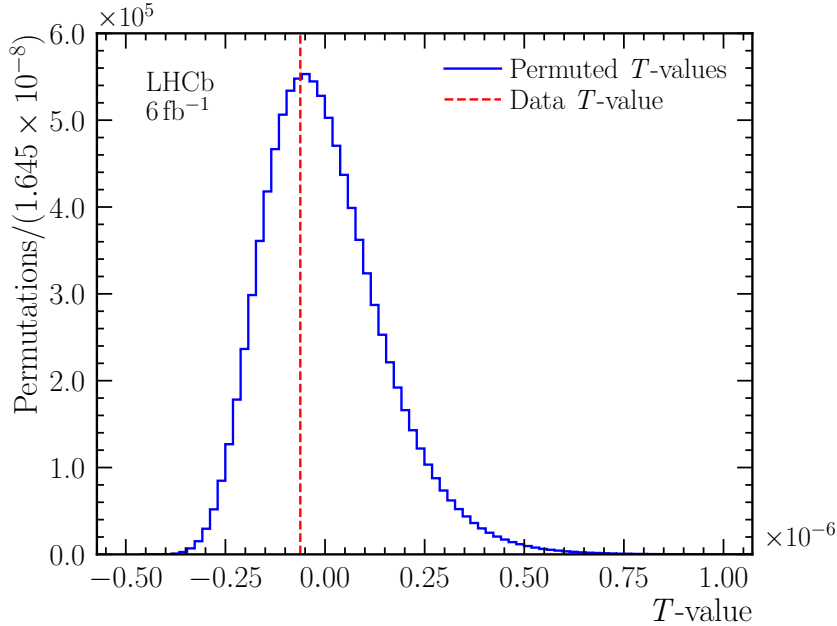


Figure 4: Distribution of T -values obtained by running the energy test over the final signal $D^0 \rightarrow \pi^- \pi^+ \pi^0$ sample (red dashed line) superimposed on the corresponding distribution for the CP -symmetry hypothesis, obtained from flavour-randomised permutations of the same data sample.

8 Results and conclusions

After comprehensive validation as discussed above, the energy test is performed in the Δm signal region for the $D^0 \rightarrow \pi^- \pi^+ \pi^0$ channel. This yields a p -value of 0.62, giving no indication of any CP violation in localised regions of the phase space. Figure 4 shows the corresponding T -value observed in data, superimposed on the expected distribution of T -values for the CP -symmetry hypothesis.

Similar cross-checks are performed as described for the control mode, including running the energy test separately for each data-taking year and hardware trigger category. All results are found to be self-consistent with no indication of systematic effects from nuisance asymmetries.

In summary, no evidence is found for CP violation in localised regions of the phase space for the decay $D^0 \rightarrow \pi^- \pi^+ \pi^0$. The analysis uses the complete data sample available in LHCb Run 2, collected during 2015–2018, containing approximately four times the signal yield of the previous energy test analysis of this channel based on data taken in Run 1 during 2012 [34]. Compared to the previous analysis, the present work benefits from a computationally more efficient energy test implementation, from a re-optimised candidate selection, and from a more comprehensive suite of data-driven cross-checks to confirm that potential nuisance asymmetries can be neglected for the current sample size.

Acknowledgements

We express our gratitude to our colleagues in the CERN accelerator departments for the excellent performance of the LHC. We thank the technical and administrative staff at the

LHCb institutes. We acknowledge support from CERN and from the national agencies: CAPES, CNPq, FAPERJ and FINEP (Brazil); MOST and NSFC (China); CNRS/IN2P3 (France); BMBF, DFG and MPG (Germany); INFN (Italy); NWO (Netherlands); MNiSW and NCN (Poland); MEN/IFA (Romania); MICINN (Spain); SNSF and SER (Switzerland); NASU (Ukraine); STFC (United Kingdom); DOE NP and NSF (USA). We acknowledge the computing resources that are provided by CERN, IN2P3 (France), KIT and DESY (Germany), INFN (Italy), SURF (Netherlands), PIC (Spain), GridPP (United Kingdom), CSCS (Switzerland), IFIN-HH (Romania), CBPF (Brazil), Polish WLCG (Poland) and NERSC (USA). We are indebted to the communities behind the multiple open-source software packages on which we depend. Individual groups or members have received support from ARC and ARDC (Australia); Minciencias (Colombia); AvH Foundation (Germany); EPLANET, Marie Skłodowska-Curie Actions, ERC and NextGenerationEU (European Union); A*MIDEX, ANR, IPhU and Labex P2IO, and Région Auvergne-Rhône-Alpes (France); Key Research Program of Frontier Sciences of CAS, CAS PIFI, CAS CCEPP, Fundamental Research Funds for the Central Universities, and Sci. & Tech. Program of Guangzhou (China); GVA, XuntaGal, GENCAT, Inditex, InTalent and Prog. Atracción Talento, CM (Spain); SRC (Sweden); the Leverhulme Trust, the Royal Society and UKRI (United Kingdom).

References

- [1] N. Cabibbo, *Unitary symmetry and leptonic decays*, Phys. Rev. Lett. **10** (1963) 531.
- [2] M. Kobayashi and T. Maskawa, *CP-violation in the renormalizable theory of weak interaction*, Prog. Theor. Phys. **49** (1973) 652.
- [3] A. D. Sakharov, *Violation of CP Invariance, C asymmetry, and baryon asymmetry of the universe*, Pisma Zh. Eksp. Teor. Fiz. **5** (1967) 32.
- [4] P. Huet and E. Sather, *Electroweak baryogenesis and standard model CP violation*, Phys. Rev. **D51** (1995) 379, arXiv:hep-ph/9404302.
- [5] A. Riotto and M. Trodden, *Recent progress in baryogenesis*, Ann. Rev. Nucl. Part. Sci. **49** (1999) 35, arXiv:hep-ph/9901362.
- [6] J. H. Christenson, J. W. Cronin, V. L. Fitch, and R. Turlay, *Evidence for the 2π Decay of the K_2^0 Meson*, Phys. Rev. Lett. **13** (1964) 138.
- [7] KTeV collaboration, A. Alavi-Harati *et al.*, *Observation of direct CP violation in $K_{S,L} \rightarrow \pi\pi$ decays*, Phys. Rev. Lett. **83** (1999) 22, arXiv:hep-ex/9905060.
- [8] NA48 collaboration, A. Lai *et al.*, *A Precise measurement of the direct CP violation parameter $Re(\epsilon'/\epsilon)$* , Eur. Phys. J. **C22** (2001) 231, arXiv:hep-ex/0110019.
- [9] BaBar collaboration, B. Aubert *et al.*, *Observation of CP violation in the B^0 meson system*, Phys. Rev. Lett. **87** (2001) 091801, arXiv:hep-ex/0107013.
- [10] Belle collaboration, K. Abe *et al.*, *Observation of large CP violation in the neutral B meson system*, Phys. Rev. Lett. **87** (2001) 091802, arXiv:hep-ex/0107061.

- [11] BaBar collaboration, B. Aubert *et al.*, *Observation of direct CP violation in $B^0 \rightarrow K^+\pi^-$ decays*, Phys. Rev. Lett. **93** (2004) 131801, arXiv:hep-ex/0407057.
- [12] Belle collaboration, Y. Chao *et al.*, *Evidence for direct CP violation in $B^0 \rightarrow K^+\pi^-$ decays*, Phys. Rev. Lett. **93** (2004) 191802, arXiv:hep-ex/0408100.
- [13] LHCb collaboration, R. Aaij *et al.*, *First observation of CP violation in the decays of B_s^0 mesons*, Phys. Rev. Lett. **110** (2013) 221601, arXiv:1304.6173.
- [14] LHCb collaboration, R. Aaij *et al.*, *Observation of CP violation in $B^\pm \rightarrow DK^\pm$ decays*, Phys. Lett. **B712** (2012) 203, Erratum *ibid.* **B713** (2012) 351, arXiv:1203.3662.
- [15] LHCb collaboration, R. Aaij *et al.*, *Observation of CP violation in two-body B_s^0 -meson decays to charged pions and kaons*, JHEP **03** (2021) 075, arXiv:2012.05319.
- [16] LHCb collaboration, R. Aaij *et al.*, *Observation of CP violation in charm decays*, Phys. Rev. Lett. **122** (2019) 211803, arXiv:1903.08726.
- [17] F. Buccella, A. Paul, and P. Santorelli, *$SU(3)_F$ breaking through final state interactions and CP asymmetries in $D \rightarrow PP$ decays*, Phys. Rev. **D99** (2019) 113001, arXiv:1902.05564.
- [18] A. Dery and Y. Nir, *Implications of the LHCb discovery of CP violation in charm decays*, JHEP **12** (2019) 104, arXiv:1909.11242.
- [19] M. Chala, A. Lenz, A. V. Rusov, and J. Scholtz, *ΔA_{CP} within the Standard Model and beyond*, JHEP **07** (2019) 161, arXiv:1903.10490.
- [20] S. Schacht and A. Soni, *Enhancement of charm CP violation due to nearby resonances*, Phys. Lett. **B825** (2022) 136855, arXiv:2110.07619.
- [21] A. J. Buras, P. Colangelo, F. De Fazio, and F. Lopalco, *The charm of 331*, JHEP **10** (2021) 021, arXiv:2107.10866.
- [22] I. Bediaga, T. Frederico, and P. Magalhaes, *Enhanced charm CP asymmetries from final state interactions*, arXiv:2203.04056.
- [23] Y. Grossman, A. L. Kagan, and Y. Nir, *New physics and CP violation in singly Cabibbo suppressed D decays*, Phys. Rev. **D75** (2007) 036008.
- [24] J. Brod, A. L. Kagan, and J. Zupan, *Size of direct CP violation in singly Cabibbo-suppressed D decays*, Phys. Rev. **D86** (2012) 014023, arXiv:1111.5000.
- [25] D. Atwood and A. Soni, *Searching for the origin of CP violation in Cabibbo suppressed D meson decays*, PTEP **2013** (2013) 093B05, arXiv:1211.1026.
- [26] Y. Grossman, A. L. Kagan, and J. Zupan, *Testing for new physics in singly Cabibbo suppressed D decays*, Phys. Rev. **D85** (2012) 114036, arXiv:1204.3557.
- [27] A. Dery, Y. Grossman, S. Schacht, and A. Soffer, *Probing the $\Delta U = 0$ rule in three body charm decays*, JHEP **05** (2021) 179, arXiv:2101.02560.




















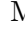


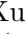
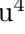
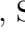









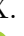







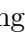





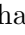


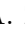

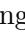

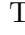




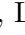




- [28] Q. Qin, H.-n. Li, C.-D. Lü, and F.-S. Yu, *Branching ratios and direct CP asymmetries in $D \rightarrow PV$ decays*, Phys. Rev. **D89** (2014) 054006, arXiv:1305.7021.
- [29] H.-Y. Cheng and C.-W. Chiang, *Revisiting CP violation in $D \rightarrow PP$ and VP decays*, Phys. Rev. **D100** (2019) 093002, arXiv:1909.03063.
- [30] H.-Y. Cheng and C.-W. Chiang, *CP violation in quasi-two-body $D \rightarrow VP$ decays and three-body D decays mediated by vector resonances*, Phys. Rev. **D104** (2021) 073003, arXiv:2104.13548.
- [31] LHCb collaboration, R. Aaij *et al.*, *Direct CP violation in charmless three-body decays of B^\pm mesons*, arXiv:2206.07622, to appear in Phys. Rev. D.
- [32] LHCb collaboration, R. Aaij *et al.*, *Measurement of the CKM angle γ with $B^\mp \rightarrow D[K^\pm \pi^\mp \pi^\mp \pi^\pm] h^\mp$ decays using a binned phase-space approach*, arXiv:2209.03692, submitted to JHEP.
- [33] LHCb collaboration, R. Aaij *et al.*, *Measurement of the time-integrated CP asymmetry in $D^0 \rightarrow K^- K^+$ decays*, arXiv:2209.03179, submitted to PRL.
- [34] LHCb collaboration, R. Aaij *et al.*, *Search for CP violation in $D^0 \rightarrow \pi^- \pi^+ \pi^0$ decays with the energy test*, Phys. Lett. **B740** (2015) 158, arXiv:1410.4170.
- [35] Y. Amhis *et al.*, *Averages of b -hadron, c -hadron, and τ -lepton properties as of 2021*, Phys. Rev. D **107** (2023) 052008, arXiv:2206.07501.
- [36] BaBar collaboration, B. Aubert *et al.*, *Search for CP violation in neutral D meson Cabibbo-suppressed three-body decays*, Phys. Rev. **D78** (2008) 051102, arXiv:0802.4035.
- [37] Belle collaboration, K. Arinstein *et al.*, *Measurement of the ratio $B(D^0 \rightarrow \pi^+ \pi^- \pi^0) / B(D^0 \rightarrow K^- \pi^+ \pi^0)$ and the time-integrated CP asymmetry in $D^0 \rightarrow \pi^+ \pi^- \pi^0$* , Phys. Lett. **B662** (2008) 102, arXiv:0801.2439.
- [38] CLEO collaboration, D. Cronin-Hennessy *et al.*, *Searches for CP violation and $\pi\pi$ S -wave in the Dalitz-Plot of $D^0 \rightarrow \pi^+ \pi^- \pi^0$* , Phys. Rev. **D72** (2005) 031102, arXiv:hep-ex/0503052, [Erratum: Phys.Rev.D 75, 119904 (2007)].
- [39] Heavy Flavor Averaging Group, Y. Amhis *et al.*, *Averages of b -hadron, c -hadron, and τ -lepton properties as of 2018*, Eur. Phys. J. **C81** (2021) 226, arXiv:1909.12524, updated results and plots available at <https://hflav.web.cern.ch>.
- [40] Belle collaboration, N. K. Nisar *et al.*, *Search for CP violation in $D^0 \rightarrow \pi^0 \pi^0$ decays*, Phys. Rev. Lett. **112** (2014) 211601, arXiv:1404.1266.
- [41] CLEO collaboration, G. Bonvicini *et al.*, *Search for CP violation in $D^0 \rightarrow K_S^0 \pi^0$ and $D^0 \rightarrow \pi^0 \pi^0$ and $D^0 \rightarrow K_S^0 K_S^0$ decays*, Phys. Rev. **D63** (2001) 071101, arXiv:hep-ex/0012054.
- [42] B. Aslan and G. Zech, *New test for the multivariate two-sample problem based on the concept of minimum energy*, Journal of Statistical Computation and Simulation **75** (2005) 109, arXiv:math/0309164.

- [43] B. Aslan and G. Zech, *Statistical energy as a tool for binning-free, multivariate goodness-of-fit tests, two-sample comparison and unfolding*, Nucl. Instrum. Meth. **A537** (2005) 626.
- [44] M. Williams, *Observing CP violation in many-body decays*, Phys. Rev. **D84** (2011) 054015, arXiv:1105.5338.
- [45] C. Parkes *et al.*, *On model-independent searches for direct CP violation in multi-body decays*, J. Phys. **G44** (2017) 085001, arXiv:1612.04705.
- [46] LHCb collaboration, R. Aaij *et al.*, *Search for CP violation in the phase space of $D^0 \rightarrow \pi^+\pi^-\pi^+\pi^-$ decays*, Phys. Lett. **B769** (2017) 345, arXiv:1612.03207.
- [47] LHCb collaboration, R. Aaij *et al.*, *Search for CP violation and observation of P violation in $\Lambda_b^0 \rightarrow p\pi^-\pi^+\pi^-$ decays*, Phys. Rev. **D102** (2020) 051101, arXiv:1912.10741.
- [48] W. Barter, C. Burr, and C. Parkes, *Calculating p-values and their significances with the Energy Test for large datasets*, JINST **13** (2018) P04011, arXiv:1801.05222.
- [49] G. Zech, *Scaling property of the statistical two-sample energy test*, arXiv:1804.10599.
- [50] T. P. S. Gillam and C. G. Lester, *Biased bootstrap sampling for efficient two-sample testing*, JINST **13** (2018) P12014, arXiv:1810.00335.
- [51] LHCb collaboration, R. Aaij *et al.*, *Measurement of CP asymmetry in $D^0 \rightarrow K^-K^+$ and $D^0 \rightarrow \pi^-\pi^+$ decays*, JHEP **07** (2014) 041, arXiv:1405.2797.
- [52] LHCb collaboration, A. A. Alves Jr. *et al.*, *The LHCb detector at the LHC*, JINST **3** (2008) S08005.
- [53] LHCb collaboration, R. Aaij *et al.*, *LHCb detector performance*, Int. J. Mod. Phys. **A30** (2015) 1530022, arXiv:1412.6352.
- [54] R. Aaij *et al.*, *Performance of the LHCb Vertex Locator*, JINST **9** (2014) P09007, arXiv:1405.7808.
- [55] P. d'Argent *et al.*, *Improved performance of the LHCb Outer Tracker in LHC Run 2*, JINST **12** (2017) P11016, arXiv:1708.00819.
- [56] M. Adinolfi *et al.*, *Performance of the LHCb RICH detector at the LHC*, Eur. Phys. J. **C73** (2013) 2431, arXiv:1211.6759.
- [57] A. A. Alves Jr. *et al.*, *Performance of the LHCb muon system*, JINST **8** (2013) P02022, arXiv:1211.1346.
- [58] R. Aaij *et al.*, *The LHCb trigger and its performance in 2011*, JINST **8** (2013) P04022, arXiv:1211.3055.
- [59] W. D. Hulsbergen, *Decay chain fitting with a Kalman filter*, Nucl. Instrum. Meth. **A552** (2005) 566, arXiv:physics/0503191.
- [60] A. Hoecker *et al.*, *TMVA: Toolkit for Multivariate Data Analysis*, PoS **ACAT** (2007) 040, arXiv:physics/0703039.

- [61] M. Pivk and F. R. Le Diberder, *SPlot: A Statistical tool to unfold data distributions*, Nucl. Instrum. Meth. **A555** (2005) 356, [arXiv:physics/0402083](#).
- [62] BaBar collaboration, B. Aubert *et al.*, *Measurement of CP violation parameters with a Dalitz plot analysis of $B^\pm \rightarrow D(\pi^+\pi^-\pi^0) K^\pm$* , Phys. Rev. Lett. **99** (2007) 251801, [arXiv:hep-ex/0703037](#).
- [63] J. Back *et al.*, *LAURA⁺⁺: A Dalitz plot fitter*, Comput. Phys. Commun. **231** (2018) 198, [arXiv:1711.09854](#).

LHCb collaboration

R. Aaij³², A.S.W. Abdelmotteleb⁵¹, C. Abellan Beteta⁴⁵, F. Abudinén⁵¹,
T. Ackernley⁵⁵, B. Adeva⁴¹, M. Adinolfi⁴⁹, P. Adlarson⁷⁷, H. Afsharnia⁹,
C. Agapopoulou⁴³, C.A. Aidala⁷⁸, Z. Ajaltouni⁹, S. Akar⁶⁰, K. Akiba³²,
P. Albicocco²³, J. Albrecht¹⁵, F. Alessio⁴³, M. Alexander⁵⁴, A. Alfonso Albero⁴⁰,
Z. Aliouche⁵⁷, P. Alvarez Cartelle⁵⁰, R. Amalric¹³, S. Amato², J.L. Amey⁴⁹,
Y. Amhis^{11,43}, L. An⁵, L. Anderlini²², M. Andersson⁴⁵, A. Andreianov³⁸,
M. Andreotti²¹, D. Andreou⁶³, D. Ao⁶, F. Archilli^{31,s}, A. Artamonov³⁸,
M. Artuso⁶³, E. Aslanides¹⁰, M. Atzeni⁴⁵, B. Audurier¹², I.B. Bachiller Perea⁸,
S. Bachmann¹⁷, M. Bachmayer⁴⁴, J.J. Back⁵¹, A. Bailly-reyre¹³,
P. Baladron Rodriguez⁴¹, V. Balagura¹², W. Baldini^{21,43}, J. Baptista de Souza Leite¹,
M. Barbeti^{22,j}, I. R. Barbosa⁶⁵, R.J. Barlow⁵⁷, S. Barsuk¹¹, W. Barter⁵³,
M. Bartolini⁵⁰, F. Baryshnikov³⁸, J.M. Basels¹⁴, G. Bassi^{29,p}, B. Batsukh⁴,
A. Battig¹⁵, A. Bay⁴⁴, A. Beck⁵¹, M. Becker¹⁵, F. Bedeschi²⁹, I.B. Bediaga¹,
A. Beiter⁶³, S. Belin⁴¹, V. Bellee⁴⁵, K. Belous³⁸, I. Belov³⁸, I. Belyaev³⁸,
G. Benane¹⁰, G. Bencivenni²³, E. Ben-Haim¹³, A. Bereznoy³⁸, R. Bernet⁴⁵,
S. Bernet Andres³⁹, D. Berninghoff¹⁷, H.C. Bernstein⁶³, C. Bertella⁵⁷, A. Bertolin²⁸,
C. Betancourt⁴⁵, F. Betti⁴³, Ia. Bezshyiko⁴⁵, J. Bhom³⁵, L. Bian⁶⁹,
M.S. Bieker¹⁵, N.V. Biesuz²¹, P. Billoir¹³, A. Biolchini³², M. Birch⁵⁶,
F.C.R. Bishop⁵⁰, A. Bitadze⁵⁷, A. Bizzeti¹², M.P. Blago⁵⁰, T. Blake⁵¹, F. Blanc⁴⁴,
J.E. Blank¹⁵, S. Blusk⁶³, D. Bobulski⁵⁴, V.B. Bocharnikov³⁸, J.A. Boelhauve¹⁵,
O. Boente Garcia¹², T. Boettcher⁶⁰, A. Boldyrev³⁸, C.S. Bolognani⁷⁵,
R. Bolzonella^{21,i}, N. Bondar³⁸, F. Borgato²⁸, S. Borghi⁵⁷, M. Borsato¹⁷,
J.T. Borsuk³⁵, S.A. Bouchiba⁴⁴, T.J.V. Bowcock⁵⁵, A. Boyer⁴³, C. Bozzi²¹,
M.J. Bradley⁵⁶, S. Braun⁶¹, A. Brea Rodriguez⁴¹, N. Breer¹⁵, J. Brodzicka³⁵,
A. Brossa Gonzalo⁴¹, J. Brown⁵⁵, D. Brundu²⁷, A. Buonauro⁴⁵, L. Buonincontri²⁸,
A.T. Burke⁵⁷, C. Burr⁴³, A. Bursche⁶⁷, A. Butkevich³⁸, J.S. Butter³²,
J. Buytaert⁴³, W. Byczynski⁴³, S. Cadeddu²⁷, H. Cai⁶⁹, R. Calabrese^{21,i},
L. Calefice¹⁵, S. Cali²³, M. Calvi^{26,m}, M. Calvo Gomez³⁹, P. Campana²³,
D.H. Campora Perez⁷⁵, A.F. Campoverde Quezada⁶, S. Capelli^{26,m}, L. Capriotti²¹,
A. Carbone^{20,g}, R. Cardinale^{24,k}, A. Cardini²⁷, P. Carniti^{26,m}, L. Carus¹⁷,
A. Casais Vidal⁴¹, R. Caspary¹⁷, G. Casse⁵⁵, M. Cattaneo⁴³, G. Cavallero²¹,
V. Cavallini^{21,i}, S. Celani⁴⁴, J. Cerasoli¹⁰, D. Cervenkov⁵⁸, A.J. Chadwick⁵⁵,
I. Chahrouh⁷⁸, M.G. Chapman⁴⁹, M. Charles¹³, Ph. Charpentier⁴³,
C.A. Chavez Barajas⁵⁵, M. Chefdeville⁸, C. Chen¹⁰, S. Chen⁴, A. Chernov³⁵,
S. Chernyshenko⁴⁷, V. Chobanova^{41,v}, S. Cholak⁴⁴, M. Chruszcz³⁵, A. Chubykin³⁸,
V. Chulikov³⁸, P. Ciambone²³, M.F. Cicala⁵¹, X. Cid Vidal⁴¹, G. Ciezarek⁴³,
P. Cifra⁴³, G. Ciullo²¹, P.E.L. Clarke⁵³, M. Clemencic⁴³, H.V. Cliff⁵⁰,
J. Closier⁴³, J.L. Cobbledick⁵⁷, V. Coco⁴³, J. Cogan¹⁰, E. Cogneras⁹,
L. Cojocariu³⁷, P. Collins⁴³, T. Colombo⁴³, A. Comerma-Montells⁴⁰, L. Congedo¹⁹,
A. Contu²⁷, N. Cooke⁵⁴, I. Corredoira⁴¹, G. Corti⁴³, B. Couturier⁴³,
D.C. Craik⁴⁵, M. Cruz Torres^{1,e}, R. Currie⁵³, C.L. Da Silva⁶², S. Dadabaev³⁸,
L. Dai⁶⁶, X. Dai⁵, E. Dall'Occo¹⁵, J. Dalseno⁴¹, C. D'Ambrosio⁴³, J. Daniel⁹,
A. Danilina³⁸, P. d'Argent¹⁹, J.E. Davies⁵⁷, A. Davis⁵⁷, O. De Aguiar Francisco⁵⁷,
J. de Boer⁴³, K. De Bruyn⁷⁴, S. De Capua⁵⁷, M. De Cian¹⁷,
U. De Freitas Carneiro Da Graca¹, E. De Lucia²³, J.M. De Miranda¹, L. De Paula²,
M. De Serio^{19,f}, D. De Simone⁴⁵, P. De Simone²³, F. De Vellis¹⁵, J.A. de Vries⁷⁵,
C.T. Dean⁶², F. Debernardis^{19,f}, D. Decamp⁸, V. Dedu¹⁰, L. Del Buono¹³,
B. Delaney⁵⁹, H.-P. Dembinski¹⁵, V. Denysenko⁴⁵, O. Deschamps⁹, F. Dettori^{27,h},

M.R.J. Williams⁵³ , R. Williams⁵⁰ , F.F. Wilson⁵² , W. Wislicki³⁶ , M. Witek³⁵ , L. Witola¹⁷ , C.P. Wong⁶² , G. Wormser¹¹ , S.A. Wotton⁵⁰ , H. Wu⁶³ , J. Wu⁷ , Y. Wu⁵ , K. Wyllie⁴³ , Z. Xiang⁶ , Y. Xie⁷ , A. Xu²⁹ , J. Xu⁶ , L. Xu³ , L. Xu³ , M. Xu⁵¹ , Q. Xu⁶ , Z. Xu⁹ , Z. Xu⁶ , Z. Xu⁴ , D. Yang³ , S. Yang⁶ , X. Yang⁵ , Y. Yang²⁴ , Z. Yang⁵ , Z. Yang⁶¹ , V. Yeroshenko¹¹ , H. Yeung⁵⁷ , H. Yin⁷ , J. Yu⁶⁶ , X. Yuan⁴ , E. Zaffaroni⁴⁴ , M. Zavertyaev¹⁶ , M. Zdybal³⁵ , M. Zeng³ , C. Zhang⁵ , D. Zhang⁷ , J. Zhang⁶ , L. Zhang³ , S. Zhang⁶⁶ , S. Zhang⁵ , Y. Zhang⁵ , Y. Zhang⁵⁸ , Y. Zhao¹⁷ , A. Zharkova³⁸ , A. Zhelezov¹⁷ , Y. Zheng⁶ , T. Zhou⁵ , X. Zhou⁷ , Y. Zhou⁶ , V. Zhovkovska¹¹ , L. Z. Zhu⁶ , X. Zhu³ , X. Zhu⁷ , Z. Zhu⁶ , V. Zhukov^{14,38} , J. Zhuo⁴² , Q. Zou^{4,6} , S. Zucchelli^{20,g} , D. Zuliani²⁸ , G. Zunica⁵⁷ .

¹ *Centro Brasileiro de Pesquisas Físicas (CBPF), Rio de Janeiro, Brazil*

² *Universidade Federal do Rio de Janeiro (UFRJ), Rio de Janeiro, Brazil*

³ *Center for High Energy Physics, Tsinghua University, Beijing, China*

⁴ *Institute Of High Energy Physics (IHEP), Beijing, China*

⁵ *School of Physics State Key Laboratory of Nuclear Physics and Technology, Peking University, Beijing, China*

⁶ *University of Chinese Academy of Sciences, Beijing, China*

⁷ *Institute of Particle Physics, Central China Normal University, Wuhan, Hubei, China*

⁸ *Université Savoie Mont Blanc, CNRS, IN2P3-LAPP, Annecy, France*

⁹ *Université Clermont Auvergne, CNRS/IN2P3, LPC, Clermont-Ferrand, France*

¹⁰ *Aix Marseille Univ, CNRS/IN2P3, CPPM, Marseille, France*

¹¹ *Université Paris-Saclay, CNRS/IN2P3, IJCLab, Orsay, France*

¹² *Laboratoire Leprince-Ringuet, CNRS/IN2P3, Ecole Polytechnique, Institut Polytechnique de Paris, Palaiseau, France*

¹³ *LPNHE, Sorbonne Université, Paris Diderot Sorbonne Paris Cité, CNRS/IN2P3, Paris, France*

¹⁴ *I. Physikalisches Institut, RWTH Aachen University, Aachen, Germany*

¹⁵ *Fakultät Physik, Technische Universität Dortmund, Dortmund, Germany*

¹⁶ *Max-Planck-Institut für Kernphysik (MPIK), Heidelberg, Germany*

¹⁷ *Physikalisches Institut, Ruprecht-Karls-Universität Heidelberg, Heidelberg, Germany*

¹⁸ *School of Physics, University College Dublin, Dublin, Ireland*

¹⁹ *INFN Sezione di Bari, Bari, Italy*

²⁰ *INFN Sezione di Bologna, Bologna, Italy*

²¹ *INFN Sezione di Ferrara, Ferrara, Italy*

²² *INFN Sezione di Firenze, Firenze, Italy*

²³ *INFN Laboratori Nazionali di Frascati, Frascati, Italy*

²⁴ *INFN Sezione di Genova, Genova, Italy*

²⁵ *INFN Sezione di Milano, Milano, Italy*

²⁶ *INFN Sezione di Milano-Bicocca, Milano, Italy*

²⁷ *INFN Sezione di Cagliari, Monserrato, Italy*

²⁸ *Università degli Studi di Padova, Università e INFN, Padova, Padova, Italy*

²⁹ *INFN Sezione di Pisa, Pisa, Italy*

³⁰ *INFN Sezione di Roma La Sapienza, Roma, Italy*

³¹ *INFN Sezione di Roma Tor Vergata, Roma, Italy*

³² *Nikhef National Institute for Subatomic Physics, Amsterdam, Netherlands*

³³ *Nikhef National Institute for Subatomic Physics and VU University Amsterdam, Amsterdam, Netherlands*

³⁴ *AGH - University of Science and Technology, Faculty of Physics and Applied Computer Science, Kraków, Poland*

³⁵ *Henryk Niewodniczanski Institute of Nuclear Physics Polish Academy of Sciences, Kraków, Poland*

³⁶ *National Center for Nuclear Research (NCBJ), Warsaw, Poland*

³⁷ *Horia Hulubei National Institute of Physics and Nuclear Engineering, Bucharest-Magurele, Romania*

³⁸ *Affiliated with an institute covered by a cooperation agreement with CERN*

³⁹ *DS4DS, La Salle, Universitat Ramon Llull, Barcelona, Spain*

- ⁴⁰ ICCUB, Universitat de Barcelona, Barcelona, Spain
- ⁴¹ Instituto Galego de Física de Altas Enerxías (IGFAE), Universidade de Santiago de Compostela, Santiago de Compostela, Spain
- ⁴² Instituto de Física Corpuscular, Centro Mixto Universidad de Valencia - CSIC, Valencia, Spain
- ⁴³ European Organization for Nuclear Research (CERN), Geneva, Switzerland
- ⁴⁴ Institute of Physics, Ecole Polytechnique Fédérale de Lausanne (EPFL), Lausanne, Switzerland
- ⁴⁵ Physik-Institut, Universität Zürich, Zürich, Switzerland
- ⁴⁶ NSC Kharkiv Institute of Physics and Technology (NSC KIPT), Kharkiv, Ukraine
- ⁴⁷ Institute for Nuclear Research of the National Academy of Sciences (KINR), Kyiv, Ukraine
- ⁴⁸ University of Birmingham, Birmingham, United Kingdom
- ⁴⁹ H.H. Wills Physics Laboratory, University of Bristol, Bristol, United Kingdom
- ⁵⁰ Cavendish Laboratory, University of Cambridge, Cambridge, United Kingdom
- ⁵¹ Department of Physics, University of Warwick, Coventry, United Kingdom
- ⁵² STFC Rutherford Appleton Laboratory, Didcot, United Kingdom
- ⁵³ School of Physics and Astronomy, University of Edinburgh, Edinburgh, United Kingdom
- ⁵⁴ School of Physics and Astronomy, University of Glasgow, Glasgow, United Kingdom
- ⁵⁵ Oliver Lodge Laboratory, University of Liverpool, Liverpool, United Kingdom
- ⁵⁶ Imperial College London, London, United Kingdom
- ⁵⁷ Department of Physics and Astronomy, University of Manchester, Manchester, United Kingdom
- ⁵⁸ Department of Physics, University of Oxford, Oxford, United Kingdom
- ⁵⁹ Massachusetts Institute of Technology, Cambridge, MA, United States
- ⁶⁰ University of Cincinnati, Cincinnati, OH, United States
- ⁶¹ University of Maryland, College Park, MD, United States
- ⁶² Los Alamos National Laboratory (LANL), Los Alamos, NM, United States
- ⁶³ Syracuse University, Syracuse, NY, United States
- ⁶⁴ School of Physics and Astronomy, Monash University, Melbourne, Australia, associated to ⁵¹
- ⁶⁵ Pontifícia Universidade Católica do Rio de Janeiro (PUC-Rio), Rio de Janeiro, Brazil, associated to ²
- ⁶⁶ Physics and Micro Electronic College, Hunan University, Changsha City, China, associated to ⁷
- ⁶⁷ Guangdong Provincial Key Laboratory of Nuclear Science, Guangdong-Hong Kong Joint Laboratory of Quantum Matter, Institute of Quantum Matter, South China Normal University, Guangzhou, China, associated to ³
- ⁶⁸ Lanzhou University, Lanzhou, China, associated to ⁴
- ⁶⁹ School of Physics and Technology, Wuhan University, Wuhan, China, associated to ³
- ⁷⁰ Departamento de Física, Universidad Nacional de Colombia, Bogota, Colombia, associated to ¹³
- ⁷¹ Universität Bonn - Helmholtz-Institut für Strahlen und Kernphysik, Bonn, Germany, associated to ¹⁷
- ⁷² Eotvos Lorand University, Budapest, Hungary, associated to ⁴³
- ⁷³ INFN Sezione di Perugia, Perugia, Italy, associated to ²¹
- ⁷⁴ Van Swinderen Institute, University of Groningen, Groningen, Netherlands, associated to ³²
- ⁷⁵ Universiteit Maastricht, Maastricht, Netherlands, associated to ³²
- ⁷⁶ Tadeusz Kosciuszko Cracow University of Technology, Cracow, Poland, associated to ³⁵
- ⁷⁷ Department of Physics and Astronomy, Uppsala University, Uppsala, Sweden, associated to ⁵⁴
- ⁷⁸ University of Michigan, Ann Arbor, MI, United States, associated to ⁶³

^a Universidade de Brasília, Brasília, Brazil

^b Central South U., Changsha, China

^c Hangzhou Institute for Advanced Study, UCAS, Hangzhou, China

^d Excellence Cluster ORIGINS, Munich, Germany

^e Universidad Nacional Autónoma de Honduras, Tegucigalpa, Honduras

^f Università di Bari, Bari, Italy

^g Università di Bologna, Bologna, Italy

^h Università di Cagliari, Cagliari, Italy

ⁱ Università di Ferrara, Ferrara, Italy

^j Università di Firenze, Firenze, Italy

^k Università di Genova, Genova, Italy

^l Università degli Studi di Milano, Milano, Italy

^m Università di Milano Bicocca, Milano, Italy

ⁿ Università di Padova, Padova, Italy

^o *Università di Perugia, Perugia, Italy*

^p *Scuola Normale Superiore, Pisa, Italy*

^q *Università di Pisa, Pisa, Italy*

^r *Università della Basilicata, Potenza, Italy*

^s *Università di Roma Tor Vergata, Roma, Italy*

^t *Università di Urbino, Urbino, Italy*

^u *Universidad de Alcalá, Alcalá de Henares, Spain*

^v *Universidade da Coruña, Coruña, Spain*

[†] *Deceased*